Original Research Article

MHD Buoyancy Flows of Cu, Al_2O_3 and TiO_2 nanofluid near Stagnation-point on a Vertical Plate with Heat Generation

Abstract. Magnetohydrodynamic mixed convection boundary layer flow of a nanofluid near the stagnation-point on a vertical plate with heat generation is investigated for both assisting and opposing flows are well thought-out. Different types of nanoparticles (Cu, Al_2O_3 and TiO_2) considering here. Using similarity approach the system of partial differential equations is transformed into ordinary differential equations which strongly depend on the magnetic parameter, buoyancy parameter, Prandtl number, heat generation parameter and volume fraction parameter. The coupled differential equations are numerically simulated using the Nactsheim-Swigert shooting technique together with Runge-Kutta six order iteration schemes. The velocity and temperature profiles are discussed and presented graphically. The comparison for dimensionless skin friction coefficient and local Nusselt number with previously published literature also take into account for the accuracy of the present analysis.

Keywords: MHD, mixed convection, nanofluid, Heat generation, stagnation-point flow

NOMENCLATURE

a, b	constant	$U(x)$	free stream velocity
B_0	magnetic induction		
C_f	Skin friction coefficient	**Greek symbols**	
C_P	specific heat at constant pressure	ν	kinematic viscosity
G_r	Grashof number	ρ	density
k	thermal conductivity	σ	conductivity of the material
M	magnetic parameter	α	thermal diffusivity
Nu_x	Local Nusselt number	β	co-efficient of thermal expansion
P	fluid pressure	λ	Buoyancy/thermal convection parameter
P_r	Prandtl number	μ	dynamic viscosity
Q	heat source parameter	η	similarity variable
Q_0	heat generation constant	τ_w	Wall shear stress
Re_x	Local Reynolds number	ψ	stream function
T	temperature at the surface	φ	volume fraction parameter
T_∞	ambient temperature as $y \to \infty$	$f'(\eta)$	dimensionless velocity
u, v	velocity components along x, y axes respectively	$\theta(\eta)$	dimensionless temperature

1. Introduction

Magneto-fluid-dynamics or hydro-magnetics is a limitless field of research which analyzed the study of the dynamics of electrically conducting fluids includes plasmas, liquid metals, and salt water or electrolytes etc. The expression magneto-hydrodynamics (MHD) is consists of three belongings such as magneto (magnetic field), hydro (liquid) and dynamics (movement of particles). As a consequence magnetic fields induce current flows in a dynamic fluid and create forces on the fluid and also adjust the magnetic field itself. The combination of the Navier-Stokes equations of fluid-mechanics and Maxwell's equations of electromagnetism consequently established MHD relations. Due to wide applications in heat exchangers, post accidental heat removal in nuclear reactors, geothermal and oil recovery, solar collectors, drying processes, building construction, etc. the Buoyancy flow [1] and heat transfer is a significant phenomenon in engineering systems. Also as conventional heat transfer fluids, including oil, water, and ethylene glycol mixture are poor heat transfer fluids, since the thermal conductivity of these fluids plays important role on the heat transfer co-efficient between the heat transfer medium and the heat transfer surface.

The effects of heat generation arise in high temperature ingredients processing operations also it can affect on heat transfer over an extending surface [2]. Choi [3] was the first who employ a technique to improve heat transfer is by using nano-scale particles in the base fluid and introduced the term of nanofluids as a novel class of fluid. As a result this type of fluids determines high thermal conductivity, significant change in properties such as viscosity and specific heat in comparison to the base fluid.

Table 1: Thermophysical possessions of the fluid and the nanoparticles.

Physical properties	**Fluid phase (water)**	**Cu**	**Al_2O_3**	**TiO_2**
C_p**(J/kgK)**	4179	385	765	686.2
ρ**(kg /m^3)**	997.1	8933	3970	4250
k**(W/mK)**	0.613	400	40	8.9538
$\alpha \times 10^{-7}$ **(m^2/ s)**	1.47	1163.1	131.7	30.7
$\beta \times 10^{-7}$ **(m^2/ s)**	21	1.67	0.85	0.9

Nanofluid-technology is now largely used in engineering and industrial applications. Due to this applications in recent years many researchers investigates some numerical and experimental analysis on nanofluids include convective instability [4] thermal conductivity [5, 6] and natural convective boundary-layer flow [7, 8]. Recently boundary layer heat-mass transfer free convection flows also in porous media of a nanofluid past a stretched sheet reported by Khan and Pop [9]. The heat transfer and fluid flow due to buoyancy forces in a partially heated enclosure using different types of nanoparticles is carried out by Oztop and Abu-Nada [10]. They have also provided the thermo physical properties of the fluid and nanoparticles as shown in Table. 1. Hamad and Pop [11] studied MHD free convection rotating flow of a nanofluid. The boundary layer nanofluid flow with MHD radiative possessions recently predicted Md. Shakhaoath Khan et al. [12] analyzed. Khan and Pop [13] analyzed boundary layer heat and mass transfer analysis past a wedge moving in a nanofluid. Very recently Tamim *et al.*[14] investigates the mixed convection boundary layer flow of a nanofluid near the stagnation-point on a vertical plate where the mixed convection flows [15, 16, 17]are characterized by the buoyancy parameter λ, whereas for assisting flow, $\lambda > 0$ and for opposing flow$\lambda < 0$. Thesame problem corresponds to forced convection flow when the buoyancy effects are negligible ($\lambda = 0$).

The present study predicting the MHD mixed convection boundary layer flow of a nanofluid near the stagnation-point on a vertical plate with heat generation for both assisting and opposing flows. And this work extended the study of Tamim *et al.*[14]. The governing equations are transformed into nonlinear ordinary differential equations which depend on the Magnetic parameter (M), buoyancy parameter (λ), Prandtl number (P_r), Heat generation parameter (Q) and volume fraction parameter (φ).The obtained nonlinear coupled ordinary differential equations are solved numerically using Nactsheim-Swigert[18] shooting iteration technique together with Runge-Kutta six order iteration schemes. The velocity and temperature distributions are discussed and presented graphically. The comparison for dimensionless skin friction coefficient and local Nusselt number with Tamim *et al.*[14] also take into account for the accuracy of the present analysis.

2. The governing equations

The steady two dimensional boundary layer mixed convection flow considered near the stagnation-point on a vertical flat plate. The physical configuration of this problem is shown in Fig. 1 [14]. No slip conditions occurs between the thermally equilibrium nanoparticles. Here the coordinate's *x*-axis is extending along the surface whereas the *y*-axis is measured normal to the surface.

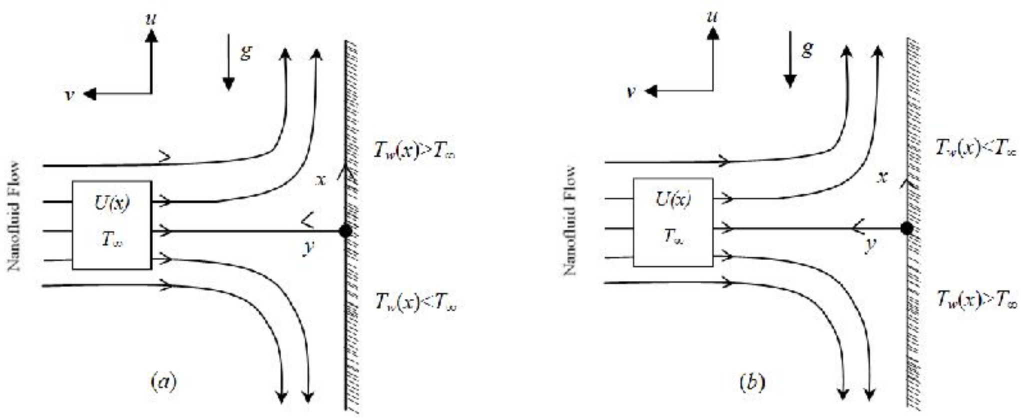

Figure 1: Physical configuration and coordinates system.

The outer boundary layerof the x-component velocity taken as $U(x) = ax$ where a is positive constants and the plate temperature taken as proportional to the distance from the stagnation-point, $T_w(x)=T_\infty+bx$, whereas b>*0*indicatesassisting flow which occurs when the superior pert of the plate is heated while the lower half of the plated is cooled. And $b<0$ indicates opposing flow which occurs if the superior pert of the plate is cooled while the lower part of the plate is heated. Thus the buoyancy force arises here to assist the main flow field.

The governing equations for the laminar two-dimensional boundary layer heat transfer flow can be written as follows;

$$\frac{\partial u}{\partial x}+\frac{\partial v}{\partial y}=0, \tag{1}$$

$$u\frac{\partial u}{\partial x}+v\frac{\partial u}{\partial y}=U\frac{dU}{dx}+\frac{\mu_{nf}}{\rho_{nf}}\left(\frac{\partial^2 u}{\partial y^2}\right)+\frac{\left[\varphi\rho_S\beta_S+(1-\varphi)\rho_f\beta_f\right]g(T-T_\infty)}{\rho_{nf}}+\frac{\sigma B_0^2}{\rho}(U-u), \tag{2}$$

$$u\frac{\partial T}{\partial x}+v\frac{\partial T}{\partial y}=\alpha_{nf}\frac{\partial^2 T}{\partial y^2}+\frac{Q_\circ}{\rho_f C_p}(T-T_\infty), \tag{3}$$

here, μ_{nf} is the viscosity of the nanofluid, α_{nf} is the thermal diffusivity of the nanofluid and ρ_{nf} is the density of the nanofluid, β_f and β_s are the thermal expansion coefficients of the base fluid and nanoparticle, respectively. The values of μ_{nf}, α_{nf} and ρ_{nf} can be written as;

$$\begin{aligned}&\mu_{nf}=\frac{\mu_f}{(1-\varphi)^{2.5}},\ \rho_{nf}=(1-\varphi)\rho_f+\varphi\rho_s,\ (\rho C_p)_{nf}=(1-\varphi)(\rho C_p)_f+\varphi(\rho C_p)_s,\\&\alpha_{nf}=\frac{k_{nf}}{(\rho C_p)_{nf}},\ \frac{k_{nf}}{k_f}=\frac{(k_s+2k_f)-2\varphi(k_f-k_s)}{(k_s+2k_f)+\varphi(k_f-k_s)},\end{aligned} \tag{4}$$

where, ρ_f and ρ_s is density of the base fluid and nanoparticle respectively, μ_f is viscosity of the base fluid, k_f and k_s is the thermal conductivity of the base fluid and nanoparticle respectively and k_{nf} is the effective thermal conductivity of the nanofluid approximated by the Maxwell-Garnett model [10].

The boundary condition for the model is;

$$\begin{aligned}&u=0,\ v=0,\ T=T_w(x)=T_\infty+bx \text{ at } y=0,\\&u=U(x)=ax,\ T\to T_\infty \text{ as } y\to\infty.\end{aligned} \tag{5}$$

In order to conquers a similarity solution to eqs. (1) to (3) with the boundary conditions (5) the following dimensionless variables are used;

$$\eta=y\sqrt{\frac{a}{\nu_f}},\ \psi=x\sqrt{a\nu_f}\,f(\eta),\ \theta=\theta(\eta)=\frac{T-T_\infty}{T_w-T_\infty} \text{ and } u=\frac{\partial\psi}{\partial y},\ v=-\frac{\partial\psi}{\partial x}. \tag{6}$$

From the above transformations the non-dimensional, nonlinear, coupled ordinary differential equations are obtained as;

$$f'''+(1-\varphi)^{2.5}(1-\varphi+\varphi\rho_S/\rho_P)\left[ff''-f'^2+1+\lambda\theta+M(1-f')\right]=0, \tag{7}$$

$$\theta''+\left(P_r\frac{(1-\varphi)+\varphi(\rho C_p)_S/(\rho C_p)_f}{k_{nf}/k_f}\right)(f\theta'-f'\theta+Q\theta)=0. \tag{8}$$

The transformed boundary conditions are as follows:

$$\left.\begin{aligned}&f=0, f'=0, \theta=1 && at\ \eta=0\\&f'=1, \theta=0 && as\ \eta\to\infty.\end{aligned}\right\} \tag{9}$$

where the notation primes denote differentiation with respect to η and the parameters are defined as Magnetic parameter $M=\frac{\sigma B_0^2}{\rho a}$, thermal convective parameter $\lambda=\frac{G_r}{\mathrm{Re}_x^2}=\frac{b[\varphi\rho_S\beta_S+(1-\varphi)\rho_f\beta_f]g}{\rho_{nf}a^2}$, local Grashof number $G_r=\frac{x^3[\varphi\rho_S\beta_S+(1-\varphi)\rho_f\beta_f]g(T_w-T_\infty)}{\rho_{nf}\nu_{nf}^2}$, local Reynolds number $\mathrm{Re}_x=\frac{xU(x)}{\nu_{nf}}$, Prandtl number $P_r=\frac{\upsilon_f}{\alpha_f}$ and heat source parameter $Q=\frac{Q_\circ}{a\rho C_p}$. The physical quantities of interest are the skin friction coefficient and the local Nusselt number can be obtained [14] as follows;

$$C_f[\mathrm{Re}_x]^{1/2}=2\frac{f''(0)}{(1-\varphi)^{2.5}},\quad Nu_x[\mathrm{Re}_x]^{-1/2}=-\frac{k_{nf}\theta'(0)}{k_f}. \tag{10}$$

3. Numerical simulation

The non-dimensional, nonlinear, coupled ordinary differential eqs. (7) and (8) with boundary conditions (9) are solved numerically using the Nactsheim and Swigert [18]shooting iteration technique together with a sixth-order Runge-Kutta iteration scheme to determine the continuity, momentum and energy as a function of the independent variable, η. In this approach, the missing (unspecified) initial condition at the initial point of the interval is assumed and the differential equation is integrated numerically asan initial value problem to the terminal point. The accuracy of the assumed missing initial condition is then verified via comparison with the computed value of the dependent variable at the terminal point with its given value there. If a difference exists, another value of the missing initial condition must be assumed and the process is repeated. This process is continued until the agreement between the calculated and the given condition at the terminal point is within the specified degree of accuracy. Extension of the iteration shell to considered system of differential eqns. is straightforward; there are two asymptotic boundary condition and hence two unknown surface conditions $f'(0)$ and $\theta(0)$.

4. Results and Discussion

The numerical values of velocity and temperature have been computed for the magnetic parameter, M, Thermal convective parameter, λ, Prandtl number, P_r heat generation parameter, Q, and volume fraction parameter, φ respectively. Among the parameters $\lambda>0$ for assisting flows, $\lambda<0$ for opposing flows and $\lambda = 0$ corresponding to forced convection when the buoyancy force is absent.Different nanofluid-particles as copper (Cu), alumina (Al_2O_3) and titania (TiO_2) are taken into account. To assess the accuracy of the numerical results the Skin friction coefficient and surface heat rate compared with previous literature [14] and shown in Table 2-4. And excellent agreement is observed from this comparison. Also a consequence has been found that the skin friction coefficient and local Nusselt number increase with increasing λ & φ.

Table 2: Comparison of the skin friction coefficient and the Nusselt number when $\lambda = 1$, $M=0$, and $Q=0$.

Nanoparticle	φ	λ=1 (Assisting flow)			
		Tamim *et al.*[14]	Present Results	Tamim*et al.*[14]	Present Results
		$[Re_x]^{1/2}C_f$	$[Re_x]^{1/2}C_f$	$[Re_x]^{1/2}Nu_x$	$[Re_x]^{1/2}Nu_x$
Cu	0.00	3.05355	3.05687	1.65242	1.66482
	0.05	3.91833	3.91987	1.87279	1.89754
	0.10	4.81536	4.81754	2.08336	2.08458
	0.15	5.77580	5.79630	2.29008	2.29145

	0.20	6.82739	6.84644	2.49642	2.49783
Al_2O_3	0.00	3.05355	3.05683	1.65242	1.66092
	0.05	3.51805	3.52584	1.80652	1.81547
	0.10	4.02763	4.02359	1.96055	1.97580
	0.15	4.59295	4.59578	2.11528	2.12254
	0.20	5.22693	5.22699	2.27145	2.28654
TiO_2	0.00	3.05355	3.05482	1.65242	1.66874
	0.05	3.53844	3.53963	1.78590	1.79872
	0.10	4.06820	4.06899	1.91667	1.92547
	0.15	4.65406	4.65546	2.04529	2.04689
	0.20	5.30940	5.31205	2.17213	2.17321

Table 3: Comparison of the skin friction coefficient and the Nusselt number when λ = 0, *M*=0, and *Q=0*.

Nanoparticle	φ	**λ = 0 (Forced convection)**			
		Tamim *et al.*[14]	Present Results	Tamim*et al.*[14]	Present Results
		$[Re_x]^{1/2}C_f$	$[Re_x]^{1/2}C_f$	$[Re_x]^{1/2}Nu_x$	$[Re_x]^{1/2}Nu_x$
Cu	0.00	2.46518	2.47584	1.57343	1.58741
	0.05	3.10770	3.11459	1.77577	1.78421
	0.10	3.76865	3.78452	1.96921	1.97710
	0.15	4.47381	4.49874	2.15931	2.16879
	0.20	5.24549	5.25568	2.34936	2.35510
Al_2O_3	0.00	2.46518	2.47412	1.57343	1.58741
	0.05	2.81753	2.82568	1.71690	1.72201
	0.10	3.20411	3.21254	1.86033	1.87405
	0.15	3.63365	3.64582	2.00450	2.01373
	0.20	4.11665	4.12658	2.15020	2.16687
TiO_2	0.00	2.46518	2.47178	1.57343	1.58957
	0.05	2.83469	2.84581	1.69742	1.69987
	0.10	3.23858	3.24410	1.81898	1.82574
	0.15	3.68615	3.69870	1.93870	1.94783
	0.20	4.18844	4.19973	2.05698	2.06547

Table 4: Comparison of the skin friction coefficient and the Nusselt number when λ = -1, *M*=0, and *Q=0*.

Nanoparticle	φ	**λ =-1 (Opposing flow)**			
		Tamim *et al.*[14]	Present Results	Tamim*et al.*[14]	Present Results
		$[Re_x]^{1/2}C_f$	$[Re_x]^{1/2}C_f$	$[Re_x]^{1/2}Nu_x$	$[Re_x]^{1/2}Nu_x$
Cu	0.00	1.82621	1.83584	1.47787	1.48741
	0.05	2.22075	2.23257	1.65618	1.66254
	0.10	2.61683	2.62250	1.82647	1.83102
	0.15	3.03459	3.05471	1.99394	1.99871

	0.20	3.49056	3.49910	2.16169	2.18457
Al_2O_3	0.00	1.82621	1.83258	1.47787	1.49542
	0.05	2.05421	2.07582	1.60756	1.61287
	0.10	2.30424	2.30871	1.73719	1.74410
	0.15	2.58292	2.59651	1.86760	1.87412
	0.20	2.89819	2.89993	1.99963	2.00478
TiO_2	0.00	1.82621	1.83247	1.47787	1.48974
	0.05	2.06795	2.07412	1.58950	1.59952
	0.10	2.33229	2.34127	1.69904	1.71243
	0.15	2.62650	2.63658	1.80712	1.81470
	0.20	2.95913	2.96524	1.91423	1.92105

Fig. 2 depicts the velocity profiles for different values of naoparticles and magnetic parameter, M when $\lambda = 2$ (assisting flow). As a result, the momentum boundary layer thickness increases. It is evident from these figures that velocity profiles satisfy the far field boundary conditions asymptotically and validated the numerical results. Fig. 3 represents the temperature profiles for different values of naoparticles and prandtl number P_r, when $\lambda = 2$ (assisting flow). It was found the temperature boundary layer decreases as Prandtl number increases.

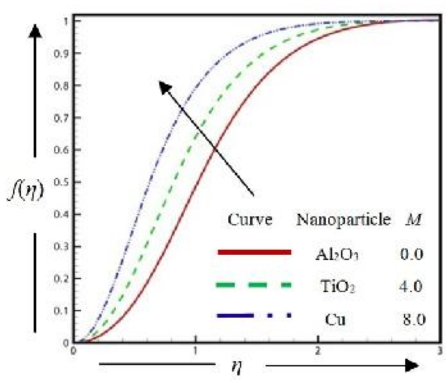

Figure 2: Velocity distribution for different types of nanoparticle and M where $\varphi=0.3$, $\lambda=2.0$, $P_r=0.71$ & $Q=1.0$

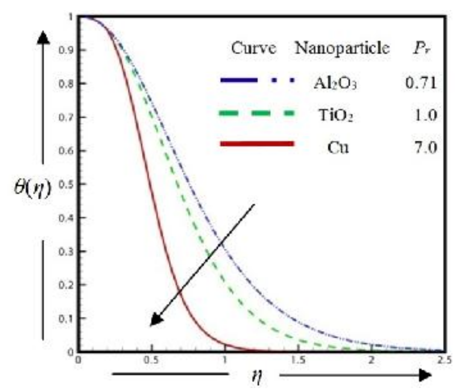

Figure 3: Temperature distribution for different types of naoparticle and P_r where $\varphi=0.3$, $\lambda=2.0$, $Q=1.0$ & $M=4.0$.

The effect of the heat generation and different nanoparicle on velocity and temperature distributions in the case of $\lambda = 0$ (forced convection) are illustrated in Fig. 4 and 5, respectively. It is observed that the momentum boundary layer thickness increases while the thermal boundary layer decreases as the heat generation growths.

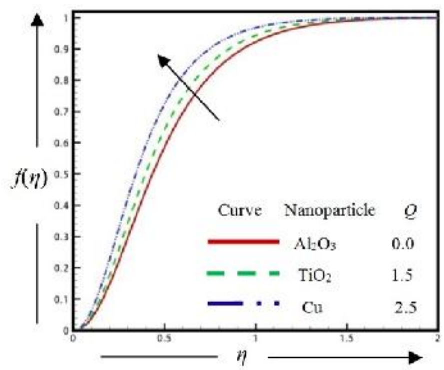

Figure 4: Velocity distribution for different types of nanoparticle and *Q* where φ*=0.3, λ =0.0, P_r=0.71 &M=4.0.*

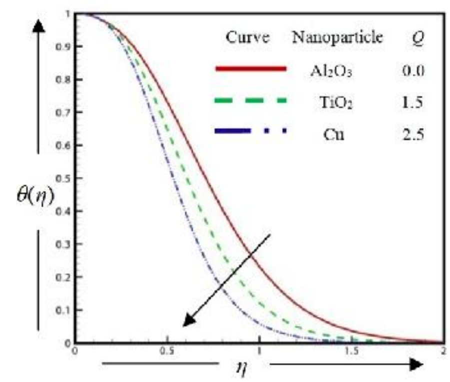

Figure 5: Temperature distribution for different types of naoparticle and *Q* where φ*=0.3, λ =0.0, P_r=0.71 & M=4.0.*

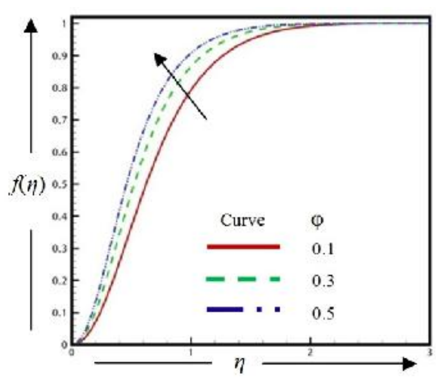

Figure 6: Velocity distribution for different types of volume fraction parameter, *φ* where *Q=1.0, λ =-2.0, P_r=0.71 & M=4.0.*

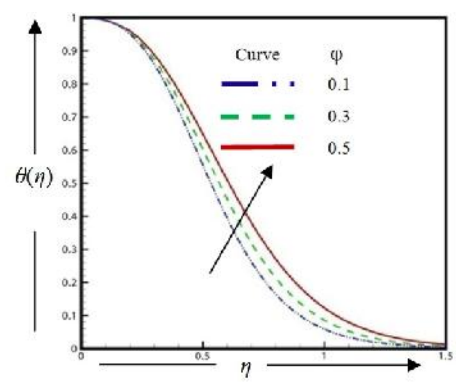

Figure 7: Temperature distribution for different types of volume fraction parameter, *φ* where *Q=1.0, λ =-2.0, P_r=0.71 & M=4.0.*

Fig. 6 show the velocity profiles for various values of the volume fraction parameter φ in the case of titania (TiO_2)-water when λ = -2 (opposing flow). It is noted that due to the fact that the presence of nano-solid-particles leads to further diminishing of the boundary layer the momentum boundary layer thickness increases with the volume fraction parameter. Figure 7 is presented to show the effect of the TiO_2 nanoparticle volume fraction on temperature distribution. From this figure, when the volume of TiO_2 nanoparticles increases, the thermal conductivity increases, and then the thermal boundary layer thickness increases progressively.

5. Conclusion

Magnetohydroynamics mixed convection boundary layer heat transfer flow of a nanofluid near the stagnation-point on a vertical plate with the effect of heat generation has been studied. Heat transfer characteristics of copper (Cu), alumina (Al_2O_3) and titania

(TiO_2) nanoparticles is observed. The momentum boundary layer thickness increases for all cases. The temperature boundary layer thickness is going down for varying different types of nanoparticle, increasing heat generation and Prandtl number respectively. But at higher volume fraction parameter the temperature boundary layer thickness rises gradually. The current study has applications in high-temperature nano-technological materials processing.

8. COMPETING INTERESTS

The authors declare that they have no competing interests.

REFERENCES

1. S. Ostrach, Natural convection in enclosures, *J. Heat Transfer*, 110 (1988) 1175–1190.
2. K. Vajravelu and A. Hadjinicalaou, Heat transfer in a viscous fluid over a stretching sheet with viscous dissipation and internal heat generation, *Int. Comm. Heat Mass Trans.*, 20 (1993) 417-430.
3. S.U.S.Choi, Enhancing thermal conductivity of fluids with nanoparticles, Development and Applications of Non-Newtonian Flows, D.A. Siginer and H. P.Wang, eds., ASME MD- vol. 231 and FED-vol. 66, USDOE, Washington, DC (United States), (1995) 99-1 05.
4. J.Y.T. Kang Ki and C.K. Choi, Analysis of convective instability and heat transfer characteristics of nanofluids, *Phys. Fluids*, 16 (2004) 2395-2401.
5. H.U. Kang, S.H. Kim and J.M. Oh, Estimation of thermal conductivity of nanofluid using experimental effective particle volume, *Exp. Heat Transfer*, 19 (2006) 181-191.
6. S.P. Jang, S.U.S. Choi, Effects of various parameters on nanofluid thermal conductivity, *ASME J. Heat Transfer.,* 129 (2007) 617-623.
7. .A. Nield and A.V. Kuznetsov, The Cheng–Minkowycz problem for natural convective boundary-layer flow in a porous medium saturated by a nanofluid, *Int. J. Heat and Mass Transfer*, 52 (2009) 5792 – 5795.
8. A.V. Kuznetsov and D.A. Nield, Natural convective boundary-layer flow of a nanofluid past a vertical plate, *Int. J. of Thermal Sci*., 49 (2010) 243 -247.
9. W.A. Khan and I. Pop, Free convection boundary layer flow past a horizontal flat plate embedded in a porous medium filled with a nanofluid, *ASME J. Heat Transfer,* 133 (2011) 157-163.
10. H.F. Oztop and E. Abu-Nada, Numerical study of natural convection in partially heated rectangular enclosures filled with nanofluids, *International Journal of Heat and Fluid Flow,* 29 (2008) 1326–1336.
11. M.A.A. Hamad and I. Pop, Unsteady MHD free convection flow past a vertical permeable flat plate in a rotating frame of reference with constant heat surface in a nanofluid, *Heat Mass Transfer*, 47 (2012) 1517-1524.
12. M.S. Khan, M.M. Alam and M. Ferdows , Effects of Magnetic field on Radiative flow of a Nanofluid past a Stretching Sheet, *Procedia Engineering Elsevier*, 56 (2013) 316-322.

13. W.A. Khan and I. Pop, Boundary Layer Flow Past a Wedge Moving in a Nanofluid, *Mathematical Problems in Engineering*, (2013) 1-7.
14. H. Tamim, P PS. Dinarvand, P PR. Hosseini, P S. Khalili and PA. Khalili, Mixed Convection Boundary-layer Flow of a Nanofluid Near Stagnation-point on a Vertical Plate with Effects of Buoyancy Assisting and Opposing Flows, *Research Journal of Applied Sciences, Engineering and Technology*, 6 (2013) 1785-1793.
15. A. Ridha, Aiding flows non-unique similarity solutions of mixed-convection boundary-layer equations, *J. Appl. Math. Phys.*, 47 (1996) 341-352.
16. J.H. Merkin and T. Mahmood, On the free convection boundary layer on a vertical plate with prescribed surface heat flux, *J. Eng. Math.*, 24 (1990) 95-107.
17. G. Wilks and J.S. Bramley,. Dual solutions in mixed convection, *P. Roy. Soc. Edinb. A,* 87 (1981) 349-358.
18. P.R. Nachtsheim and P. Swigert, Satisfaction of the asymptotic boundary conditions in numerical solution of the system of non-linear equations of boundary layer type, *NASA*, TND-3004, 1965.